

Functional relevance based on the continuous Shapley value

Pedro Delicado and Cristian Pachón-García
Departament d'Estadística i Investigació Operativa
Universitat Politècnica de Catalunya

November 28, 2024

Abstract

The presence of Artificial Intelligence (AI) in our society is increasing, which brings with it the need to understand the behaviour of AI mechanisms, including machine learning predictive algorithms fed with tabular data, text, or images, among other types of data. This work focuses on interpretability of predictive models based on functional data. Designing interpretability methods for functional data models implies working with a set of features whose size is infinite. In the context of scalar on function regression, we propose an interpretability method based on the Shapley value for continuous games, a mathematical formulation that allows to fairly distribute a global payoff among a continuous set players. The method is illustrated through a set of experiments with simulated and real data sets. The open source Python package `ShapleyFDA` is also presented.

Keywords: Interpretability, explainability, functional data analysis, Shapley value, continuous game theory, machine learning, artificial intelligence.

1 Introduction

Technological advances in recent years have affected data analysis significantly. For instance, modern smart watches are able to monitor health indicators sampling data several times per minute (Masoumian Hosseini et al. 2023). This way of obtaining data leads to treat them as if they were functions depending on a continuous argument (time, wavelength, etc.). Thus, in turns, allows us to use tools from Functional Analysis to explore that data.

Functional Data Analysis (Ramsay and Silverman 2005), or FDA for short, is a branch of Statistics whose theoretical foundations come from Functional Analysis (Horváth and Kokoszka 2012; Kokoszka and Reimherr 2017). As a brief summary, FDA considers an observation to be a function

and a sample to be a collection of functions (known as *functional data set*). Its goals are essentially the same as those of any other branch of Statistics, namely, to analyse data, to represent and display them, to study the relationship between an input variable and an outcome, and so forth.

In particular, elements from machine learning (ML), understood in a broad sense, can be found in FDA. Generally speaking, given a data set of functional data (considered as the set of explanatory variables, or feature set) and a response variable (or target), one aims at finding the best mapping between the feature set and the target. We precisely state the problem of machine learning for FDA in Section 2.1.

The application of machine learning algorithms as predictive tools is likewise a topic of interest within the field of FDA (Yao, Mueller, and Wang 2021; Rao and Reimherr 2023). Given the enormous flexibility inherent in some of these models, they are treated as black-boxes. Consequently, interpreting them is a challenging endeavour. This is a recognised issue within the field of machine learning (Barredo Arrieta et al. 2020).

In this work we present a methodology, based on Game Theory, which is designed to provide interpretability to machine learning models for FDA. Our proposal can explain any kind of model (i.e., it is *agnostic* to the underlying model), providing a *global* explanation (see, for instance, Biecek and Burzykowski 2021 for details about how interpretability methods are classified). To the best of our knowledge, this is the first work that addresses global interpretability for prediction models in the context of FDA.

The structure of this paper is as follows: Section 2 offers a brief introduction to FDA as well as to interpretable machine learning. Section 3 is devoted to the elements of Game Theory on which our proposal is based, in particular the Shapley value for continuous games. Our interpretability framework is detailed in Section 4, where we also describe the accompanying open source Python package (Python Core Team 2019). In order to study and analyse this proposal, we conduct a set of simulations, presented in Section 5, which also includes a real data example. Conclusions are provided in Section 6. Finally, certain technical material and extra outputs from simulations are deferred to the annexes.

2 Background

This section introduces and contextualises those fields that facilitate the development of this proposal. On the one hand, in Section 2.1, we provide an overview to the main aspects related to the Functional Data Analysis concerning to the regression problem. On the other hand, Section 2.2 summarises the topic of Interpretable Machine Learning in the context of multiple regression problem.

It is noteworthy that an examination of the intersection between Func-

tional Data Analysis and Interpretable Machine Learning reveals a limited corpus of existing literature. In this sense, the only work found is the recent publication of Carrizosa et al. 2024, to which we come back later.

2.1 Functional Data Analysis

This section is intended to provide a summary of FDA as well as to introduce the notation used throughout this work. Ferraty and Vieu (2006) define a *functional random variable* as a random variable \mathcal{X} taking values in an infinite dimensional space (or functional space). An observation (or realisation) \mathcal{X} of \mathcal{X} is called a *functional data*.

A functional data set $\mathcal{X}_1, \dots, \mathcal{X}_m$ is the observation/realisation of m functional random variables $\mathcal{X}_1, \dots, \mathcal{X}_m$ identically distributed as \mathcal{X} . Let $I = [a, b] \subseteq \mathbb{R}$, usually we work with data that are elements of

$$L^2(I) = \left\{ g : I \rightarrow \mathbb{R}, \text{ s.t. } \int_I g(t)^2 dt < \infty \right\}.$$

Therefore, we refer to \mathcal{X} or $\mathcal{X}(t)$ interchangeably (and the same applies to $\mathcal{X}_1, \dots, \mathcal{X}_m$).

In practise, the functional data $\mathcal{X}_j(t)$ are not available for all t in the interval $[a, b]$, but only for a finite grid $\{t_1, \dots, t_T\}$ with $t_d < t_{d+1}$. One way of representing the observed functional data is by means of a matrix \mathbf{X} of size $m \times T$, where $x_{jt} = \mathcal{X}_j(t)$, $j \in \{1, \dots, m\}$ and $t \in \mathcal{T} = \{t_1, \dots, t_T\}$.

Most of statistical techniques of multivariate analysis have been adapted to FDA. Therefore, we can find the mean function $\mu(t) = \mathbb{E}[\mathbf{X}(t)]$, the covariance function $\sigma(t, u) = \mathbb{E}[\mathbf{X}(t)\mathbf{X}(u)] - \mu(t)\mu(u)$ or even more advanced elements such as dimensionality reduction (Functional Principal Component Analysis or Functional Multidimensional Scaling) among others (Hall, Poskitt, and Presnell 2001; Hall, Müller, and Wang 2006).

Regarding regression problems, we differentiate three ways to approach this issue, which depend on the type of data: (1) scalar response on functional regressor, (2) functional response on scalar regressor and (3) functional response on functional regressor. This work focuses on modelling as a scalar response on a functional predictor.

Specifically, let (\mathcal{X}, Y) be a pair of random variables, where $Y \in \mathbb{R}$ and $\mathcal{X} \in L^2(I)$, the goal is to obtain $f : L^2(I) \rightarrow \mathbb{R}$ such that minimises $\mathbb{E}[(f(\mathcal{X}) - Y)^2]$. Usually a training data set $\{(\mathcal{X}_j, y_j)\}_{j=1}^m$ is provided with the goal of looking for f . Recall that \mathcal{X}_j is called *input variable/feature*, y_j *output variable/target* and f *machine learning model* or *prediction model*. The linear model is probably the simplest approach to regression. We say that (\mathcal{X}, Y) follows a *functional linear regression model* if

$$Y = \alpha + \int_I \mathcal{X}(t)\beta(t)dt + \epsilon,$$

where ϵ is a random term (with 0 mean and variance σ^2) independent of \mathcal{X} , $\alpha \in \mathbb{R}$ is a scalar coefficient and $\beta(t)$, $t \in I$, is a functional parameter.

2.2 Interpretable machine learning

Breiman (2001) identifies two distinct cultures within the field of data analysis: the modeling culture, based on statistical inference, and the prediction culture, focused on machine learning techniques. In addition, Breiman (2001) points out a potential trade-off between predictive ability and interpretability of models. The predictive accuracy of machine learning algorithms, such as neural networks or random forests, often exceeds that of statistical models, such as linear or logistic regression. However, statistical models provide a simpler understanding of the relationship between the response variable and the input variables. In fact, machine learning algorithms are often referred to as “black boxes” because of their inability to provide understandable explanations of the reasons behind their predictions. Nevertheless, Breiman (2001) calls for the development of procedures that would allow for better interpretation of algorithmic models without compromising their predictive ability.

In the last two decades, a powerful research line (known as Interpretable Machine Learning, IML, or eXplainable Artificial Intelligence, XAI) has been developed to provide interpretability tools to algorithmic models. This vast literature has given rise to a considerable number of review papers (see for instance, Barredo Arrieta et al. 2020) and three monographs on IML/XAI: Molnar (2022), Biecek and Burzykowski (2021) and Masis (2021), as well as many functions and packages in `R` and `Python`.

In IML/XAI a distinction is done between *global* and *local* interpretability. On the one hand, global interpretability tools measure the importance or relevance of each explanatory variable in the prediction process over their whole support. On the other hand, local interpretability tools provide meaningful explanations of why the prediction model returns a certain estimated response for a given individual, identified with a particular combination of the predicting variables values.

It is also relevant to classify IML/XAI methods as model-specific or model-agnostic. The first category includes interpretability methods that are designed to interpret a particular prediction algorithm (such as random forests or neural networks), exploiting its internal structure for interpretation. In contrast, model-agnostic interpretability methods can be applied to any prediction model. They only need to evaluate the prediction model on data from the training or test sets, or perturbations of either, and do not have access to the internal structure of the prediction model.

In this paper, we are interested in global model-agnostic interpretability methods. In the usual framework of a prediction problem with p explanatory variables and one response to which a prediction model (from Statistics or

from Machine Learning) has been fitted, global model-agnostic methods provide a relevance measure for each predictor.

The most natural way to do this is *leave-one-covariate-out* (LOCO), and it has been used in multiple linear regression for decades. Two prediction models are fitted (one with all the predictors and the other with one predictor omitted) and their prediction errors are compared: the more different they are, the more important the omitted predictor is. The main drawback of LOCO is that it requires fitting p additional models, each with $(p - 1)$ predictors. Therefore, strictly speaking, LOCO is not model-agnostic.

In Breiman (2001), a permutation-based approach is used to define variable importance for any prediction model when a test sample is available. The average prediction error for the test sample is compared with the same measure when the test sample is modified randomly permuting the values of a specific explanatory variable. The larger that difference, the more important is the permuted variable. Despite its popularity, using random permutations for interpreting black box prediction algorithms has received numerous criticisms (see, for instance, Hooker and Mentch, 2019), mainly when the predictors are moderate or highly correlated.

Delicado and Peña (2023) propose an alternative approach. First, they fit the model with all the explanatory variables in the training sample. Then, they measure the individual relevance of each explanatory variable by comparing the predictions of the model in the test set with those obtained when an explanatory variable in the test set is replaced by its *ghost variable*, defined as the conditional expectation of that variable given the values of the other explanatory variables. Delicado and Peña (2023) show that, in linear models, the proposed measure gives results similar to LOCO (with a lower computational cost and maintaining the model-agnostic character) and outperforms random permutations.

A different line of work in global model-agnostic relevance measure has been based on the Shapley value, a concept coming from Game Theory. We devote Section 3 entirely to this approach, which is the one we follow in Section 4 to develop our proposal.

The concept of feature importance is closely related to that of *variable selection* (Barber and Candès 2015; Barber and Candès 2019; Delicado and Peña 2023), in that only those features that are relevant must be included in an eventual prediction model. This approach avoids the selection of irrelevant or non-contributory features, which could eventually compromise the quality of a prediction model. Note that feature selection does not require model specification because the relationships between the explanatory variables and the target are examined directly, without the mediation of any particular prediction model. In Section 4.2 we explore two approaches that address the issue of variable selection in functional prediction.

As mentioned before, Carrizosa et al. 2024 is the only paper devoted to interpretability in functional data regression models. The authors address

the issue of local feature importance using counterfactual analysis for functional data. So, their goal is to explain (or rank) the features in a neighbourhood of a given individual, with functional observations $\mathcal{X}_0(t)$. The method is presented in the context of (multiclass) classification. The work aims at obtaining a counterfactual explanation $\mathcal{X}(t)$, which is an artificial functional data, by combining existing instances in the dataset, called *prototypes*. To achieve it, an optimisation problem is formulated, taking into account that the cost of perturbing $\mathcal{X}_0(t)$ to obtain $\mathcal{X}(t)$ must be minimal.

3 Interpretability based on game theory

This section is devoted to connecting the Shapley value for finite games, a concept from Game Theory, and interpretability for multivariate data. We also introduce how the Shapley value is considered when the game is continuous. This serves as a theoretical framework to develop our proposal, which is explained in Section 4.

3.1 Finite games

In this Section we follow Winter (2002) to present the Shapley value. The original work can be found in Shapley (1953). Given a set of players $N = \{1, \dots, n\}$, a game is a function $\nu : 2^N \rightarrow \mathbb{R}^+$, where 2^N is the set of all subsets of N and $\nu(\emptyset) = 0$. The mapping ν is known as the *payoff function* and $\nu(S)$ is interpreted as the payoff the coalition S receives for having played that game.

Let \mathcal{Q}_N be the space of all possible games with players in N . A *value* is an operator $\varphi : \mathcal{Q}_N \rightarrow (\mathbb{R}^+)^n$ that assigns to each game a vector of length n , $\varphi(\nu) = \varphi_\nu \in (\mathbb{R}^+)^n$, where the i -th component of the vector, $\varphi_{\nu,i}$ (or φ_i whenever the game can be omitted), represents the value of the player i when playing game ν . Shapley defines a set of axioms and proves that there is a unique value satisfying the axioms, being the following ones:

- **Efficiency:** the first axiom states that the sum of all the values must be equal to the total payoff:

$$\sum_{i=1}^n \varphi_i = \nu(N).$$

- **Symmetry:** first, we need to define the symmetric property. Players $i, i' \in N$ are said to be *symmetric* with respect to the game ν if for each $S \subset N$ such that $i, i' \notin S$, $\nu(S \cup \{i\}) = \nu(S \cup \{i'\})$. If i and i' are symmetric, then $\varphi_i = \varphi_{i'}$.
- **Dummy:** player i is a *dummy player* (with respect to the game ν) if for every $S \subset N$, $\nu(S \cup \{i\}) - \nu(S) = 0$. If player i is a dummy player, then $\varphi_i = 0$.

- **Additivity:** $\varphi(\nu + \omega) = \varphi(\nu) + \varphi(\omega)$, where ν and ω are games and game $\nu + \omega$ is defined as $(\nu + \omega)(S) = \nu(S) + \omega(S)$.

Theorem 1 (Shapley value, Shapley 1953). *There is a unique value satisfying the previous properties and it is given by*

$$\varphi_{\nu,i} = \frac{1}{n!} \sum_{\pi \in \mathcal{P}} [\nu(p_\pi^i \cup \{i\}) - \nu(p_\pi^i)], \quad (1)$$

where \mathcal{P} is the set of all permutations of the set N , π is a permutation and $p_\pi^i = \{j : \pi(i) > \pi(j)\}$ is the set of players preceding player i in the order π .

The quantity $[\nu(p_\pi^i \cup \{i\}) - \nu(p_\pi^i)]$ is the marginal contribution of player i to the coalition p_π^i and its Shapley value, $\varphi_{\nu,i}$, is the average of these marginal contributions over the possible different permutations of the set N .

3.2 Interpretability based on finite games

Consider a multiple linear regression model with response \mathbf{y} and p explanatory variables (or, equivalently, features) $\mathbf{x}_1, \dots, \mathbf{x}_p$, where $\mathbf{y}, \mathbf{x}_i \in \mathbb{R}^m$. Let $\bar{y} = 1/m \sum_{j=1}^m y_j$ and let \hat{y}_j be the j -th fitted value by ordinary least squares (OLS). The coefficient of determination is defined as

$$R^2 = 1 - \frac{\sum_{j=1}^m (y_j - \hat{y}_j)^2}{\sum_{j=1}^m (y_j - \bar{y})^2}$$

and it is a commonly used measure of the overall quality of the estimated model. It is also well known that R^2 is equal to the squared sampling correlation coefficient between the observed responses y_j and the fitted values \hat{y}_j . When the p explanatory variables are uncorrelated, it can be proved that

$$R^2 = \sum_{i=1}^p R_i^2,$$

where R_i^2 is the coefficient of determination in the simple linear regression of \mathbf{y} against the i -th explanatory variable \mathbf{x}_i fitted by OLS. Therefore, R_i^2 is the contribution of \mathbf{x}_i to the global quality measure R^2 , and it is a good measure of the relevance of \mathbf{x}_i in the model.

The preceding decomposition of R^2 is not applicable in the presence of correlated explanatory variables. Lipovetsky and Conklin (2001) propose an alternative decomposition based on the Shapley value. Specifically, the authors propose to consider the p explanatory variables as the set of players and the game ν as the coefficient of determination R^2 . Consequently, $\nu(S)$ is the coefficient of determination $R^2(S)$ in the regression of \mathbf{y} against the variables belonging to S fitted by OLS.

Therefore, the Shapley value of this game is a fair distribution of the total R^2 among the p predictors: $R^2 = \sum_{i=1}^p \varphi_{\nu,i}$, and $\varphi_{\nu,i}$ measures the importance of the i -th regressor in the model. Given that the exact computation of Shapley values is quite time intensive, the authors suggest to average over a moderate number of random permutations of the explanatory variables.

Feldman (2005) extends the use of the Shapley value to parametric statistical or econometric models, as a measure of the relative importance of a variable. Cohen et al. (2007) propose to use the Shapley value as global measure of variable relevance in classification problems using any prediction model (or algorithm). They propose to use the accuracy in a test set as the game ν .

3.3 Continuous games

The primary objective of this work is to incorporate interpretability within the context of FDA. Therefore, it is considered to extend the previous relevance measure based on the Shapley value to prediction models with scalar response and a functional regressor. In this context, the set of players is infinite, or, equivalently, the game becomes continuous. Consequently, the Shapley value must be defined for continuous games, also known as games with a *continuum of players* (Shapley 1961; Aumann 1964). There exists a collection of publications devoted to this topic (Kannai 1966; Aumann and Shapley 1974; Hart and Neyman 1988; Neyman 1994, among others). Obtaining the Shapley value for continuous games is not as direct as in the finite case, since a slightly more extensive theory is needed.

Let $I = [0, 1]$ and $\mathcal{B} = \mathcal{B}(I)$ be the associated Borel σ -algebra. A (continuous) *game* is a function $\nu : \mathcal{B} \rightarrow \mathbb{R}^+$ such that $\nu(\emptyset) = 0$. I is called *the set of players*, \mathcal{B} *the set of coalitions*, (I, \mathcal{B}) *the space of players* and ν *the payoff function*. Although we work with $I = [0, 1]$, the forthcoming development is valid for any interval $[a, b] \subset \mathbb{R}$.

A game is said *monotonic* if $T \subset S$ implies $\nu(T) \leq \nu(S)$. Let Q be a collection of monotonic games in (I, \mathcal{B}) . Q is a *linear space* over (I, \mathcal{B}) if $\nu_1 + \nu_2 \in Q$ for any ν_1 and ν_2 , both in Q . An *automorphism* in (I, \mathcal{B}) is a one-to-one measurable function θ from I onto I with θ^{-1} measurable. Let \mathcal{G} be the group of automorphisms of (I, \mathcal{B}) . Given a game ν , an automorphism $\theta \in \mathcal{G}$ defines a new game from ν : $(\theta_*\nu)(S) = \nu(\theta(S))$ for all $S \in \mathcal{B}$. Q is *symmetric* if $\theta_*\nu \in Q$ for all $\nu \in Q$ and all $\theta \in \mathcal{G}$.

A measure μ on (I, \mathcal{B}) is a monotonic game with the property of σ -additivity: for all countable collections $\{E_j\}_{j \geq 1}$ of pairwise disjoint sets in \mathcal{B} , $\mu(\cup_{j \geq 1} E_j) = \sum_{j \geq 1} \mu(E_j)$. Let \mathcal{M} be the set of measures defined on (I, \mathcal{B}) . Note that \mathcal{M} itself is a symmetric and linear subset of monotonic games.

A *value* on a linear symmetric space of monotonic games Q is a mapping $\psi : Q \rightarrow \mathcal{M}$ satisfying the following properties (Aumann and Shapley 1974,

page 16):

- **Efficiency:** $\forall \nu \in Q [\psi(\nu)](I) = \nu(I)$.
- **Symmetry:** $\forall \theta \in \mathcal{G} \forall \nu \in Q \theta_* \psi(\nu) = \psi(\theta_* \nu)$.
- **Linearity:** $\forall \nu_1, \nu_2 \in Q, \forall \alpha, \beta \in \mathbb{R}^+, \psi(\alpha \nu_1 + \beta \nu_2) = \alpha \psi(\nu_1) + \beta \psi(\nu_2)$.

While the concepts of efficiency and linearity are relatively straightforward to interpret, the notion of symmetry may be more abstract. According to Aumann and Shapley (1974), “*the value does not depend on how the players are named*”. This property states that the value of ν is, essentially, preserved by automorphisms.

In Aumann and Shapley (1974), the authors prove that, under certain sets of assumptions on the linear symmetric space Q of monotonic games defined on (I, \mathcal{B}) , there exists a unique value ψ satisfying the efficiency, symmetry and linearity properties. Nevertheless, deriving a formula in the continuous games context is not as straightforward as it is in the finite case. The literature referenced at the beginning of this section presents two distinct methodologies for addressing this issue. The first one, known as *the axiomatic approach*, considers only a very specific subset of games for which a closed formula can be found. Further details are provided in Section 3.2 of Neyman (1994).

The second approach, *the asymptotic approach*, considers a given continuous game as the limit of a sequence of finite games. This, in turns, allows to compute the sequence of (finite) Shapley values. Therefore, the limit value for that sequence is the Shapley value for the continuous game. We provide details about this approach below.

We consider to use the asymptotic approach because it is not as restrictive as the axiomatic approach. Our development is based on Kannai (1966) and Neyman (1994). Let $\nu : \mathcal{B} \rightarrow \mathbb{R}^+$ a game, let $\mathcal{I} = \{I_1, \dots, I_q\}$ a partition of I , let Π the σ -algebra generated by \mathcal{I} , let ν_Π the game restricted to Π , i.e. $\nu_\Pi : \Pi \rightarrow \mathbb{R}^+$ and $\nu_\Pi(S) = \nu(S) \forall S \in \Pi$. As ν_Π is a finite game, the Shapley value described in Section 3.1, $\varphi(\nu_\Pi)$, can be obtained.

In order to define the limit value, we need to consider a collection of finer and finer partitions. Let $S \in \mathcal{B}$, a *S-admissible* sequence is an increasing sequence of subalgebras $(\Pi_j)_{j \in \mathbb{N}}$ with $S \in \Pi_1 \subset \Pi_2 \subset \dots \subset \Pi_k \subset \dots$ such that $\cup_{j \in \mathbb{N}} \Pi_j$ generates \mathcal{B} . $\psi(\nu)$ is *the asymptotic value of ν* if and only if for every $S \in \mathcal{B}$ and any *S-admissible* sequence $(\Pi_j)_{j \in \mathbb{N}}$, $\lim_{j \rightarrow \infty} [\varphi(\nu_{\Pi_j})](S) = [\psi(\nu)](S)$. Under certain conditions, it can be proved that the limit exists, it is unique and it satisfies the properties previously described (Neyman 1994). Therefore, under those conditions, the value for a continuous game can be obtained as the limit of the Shapley value for finite games.

4 Relevance based on the continuous Shapley value

In this section, we present a framework for defining a relevance function for machine learning models with functional predictors. The goal is to rank the points t in the interval $I = [0, 1]$ according to their importance when predicting the response variable. We make use of the asymptotic approach described in Section 3.3. In addition, we adapt our proposal to perform feature selection.

4.1 Feature importance

We start by assuming that a test data set is available: $(\mathcal{X}_j, y_j), j \in \{1, \dots, m\}$, where $\mathcal{X}_j \in L^2(I)$ and $y_j \in \mathbb{R}$. Additionally, it can be assumed that one has access to an already trained prediction model, $f : L^2(I) \rightarrow \mathbb{R}$, and that the data used to train such a model are independent from the test data. This work focuses on the regression context, but it can be easily adapted to the classification setup.

One of the key elements is how to define the game $\nu : \mathcal{B} \rightarrow \mathbb{R}^+$ which will allow us to find the relevance function. Let $S \in \mathcal{B}$, roughly speaking $\nu(S)$ should be the proportion of variability of $\mathbf{y} = (y_1, \dots, y_m)^\top$ in the test sample explained by the prediction model f when only the information of S is considered.

A first attempt could be to retrain the model only considering the points $t \in S$, but this strategy would eventually be computationally very expensive as it would need to be performed for each $S \in \mathcal{B}$. This strategy has certain similarities with the LOCO approach to relevance features in prediction models with a finite number of predictors, described in Section 2.2. There, we have reported that Delicado and Peña (2023) overcome the LOCO issues using ghost variables: the conditional expectation of one feature, given the rest of them. An analogous approach is employed in this work.

Concretely, we propose the creation of a new data set in which the data from $t \in S$ are retained while the remaining data are inferred from S , the new data set is created using the conditional expectation, that is,

$$\tilde{\mathcal{X}}_j^S(t) = \mathcal{X}_j(t) \cdot \mathbb{1}_S(t) + \dot{\mathcal{X}}_j(t) \cdot \mathbb{1}_{S^c}(t), \quad (2)$$

with

$$\dot{\mathcal{X}}_j(t) = \mathbb{E}(\mathcal{X}(t) \mid \{\mathcal{X}(u) = \mathcal{X}_j(u) : u \in S\}),$$

where $S^c = I \setminus S$ and $j \in \{1, \dots, m\}$. This way, the functions $\tilde{\mathcal{X}}_j^S(t)$ are evaluated in all $t \in I$ and they can be used as arguments of the already trained prediction model f . Note that conditional expectation is computed under the assumption that \mathcal{X} is a Gaussian process. More details about how this estimation is done is provided in Appendix C.

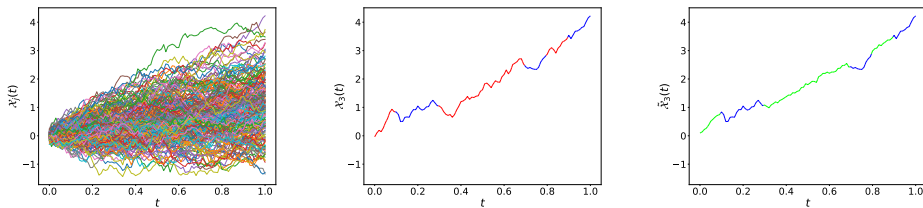


Figure 1: Left: functional data set. Middle: one functional data. The blue (respectively, red) indicates intervals in S (resp., S^c) where the functional data is known (resp., unknown). Right: reconstructed function, where the values of the functional data for the intervals in S^c (in green) are computed as their conditional expectation given the values at the intervals in S .

Next, we define $\tilde{y}_j^S = f(\tilde{\mathcal{X}}_j^S)$, $j \in \{1, \dots, m\}$, and $\nu(S)$ is defined as the coefficient of determination, computed as

$$\nu(S) = R^2(S) = 1 - \frac{\sum_{j=1}^m (y_j - \tilde{y}_j^S)^2}{\sum_{j=1}^m (y_j - \bar{y})^2},$$

where \bar{y} is the average of the target (or response) in the test set.

Figure 1 shows an example of how the new data set is obtained. On the left part of the figure, there is a data set containing 100 functions $\mathcal{X}_j(t)$ $j \in \{1, \dots, 100\}$ ($m = 100$). The middle plot is one of that functions. The intervals that are part of S are depicted in blue, whereas in red those that are part of S^c . On the rightmost side of the figure, it is shown the reconstructed functions $\tilde{\mathcal{X}}_j^S(t)$, where the green colour is used for those intervals for which conditional expectation has been used.

Recall that our goal is to make use of the asymptotic approach to compute the Shapley value of the game ν . Therefore, let $\mathcal{I} = \{I_1, \dots, I_n\}$ be a partition of $I = [0, 1]$, where $I_i = [a_i, b_i)$, $a_i < b_i$, for $i \in \{1, \dots, n-1\}$ and $I_n = [a_n, b_n]$, and let Π be the σ -algebra generated by \mathcal{I} . In the context of Game Theory, \mathcal{I} (or, equivalently, $N = \{1, \dots, n\}$) can be conceived as the set of players. Therefore, we can define the finite game $\nu_\Pi : \Pi \rightarrow \mathbb{R}^+$ as the previous game ν restricted to Π .

The objective is to compute the Shapley value for a given subset I_i (player i) using the formula stated in Theorem 1. Let \mathcal{P} the set of all permutations of \mathcal{I} , let $\pi \in \mathcal{P}$ and let p_π^i the set of players preceding i in π . By employing Equation (2), one can obviate the necessity of retraining a model for each distinct permutation.

In this context, the role of S is assumed by p_π^i (and the role of S^c is assumed by $\mathcal{I} \setminus p_\pi^i$). This, in turn, allows to compute $\nu_\Pi(p_\pi^i)$. The same line of reasoning can be applied to the case of $p_\pi^i \cup I_i$. Using the Shapley value

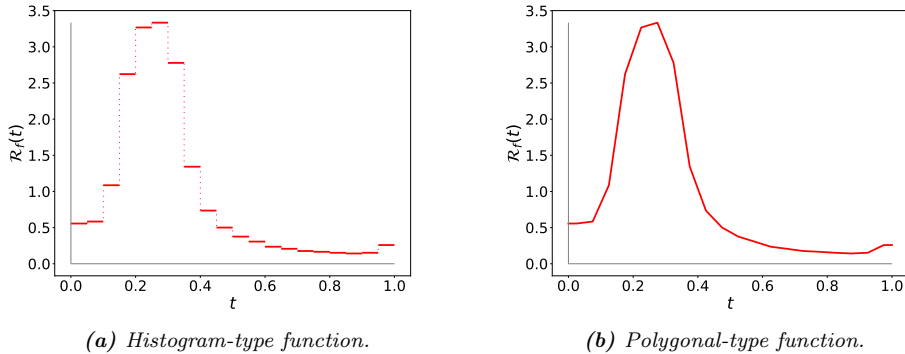


Figure 2: Example of a Shapley value function.

for finite games, the relevance of the interval I_i is given by

$$\begin{aligned}
 \varphi_{\nu,i} &= \frac{1}{n!} \sum_{\pi \in \mathcal{P}} [\nu_{\Pi}(p_{\pi}^i \cup I_i) - \nu_{\Pi}(p_{\pi}^i)] \\
 &= \frac{1}{n!} \sum_{\pi \in \mathcal{P}} [R^2(p_{\pi}^i \cup I_i) - R^2(p_{\pi}^i)].
 \end{aligned} \tag{3}$$

In practice, as the size of the set of all permutations \mathcal{P} could be extremely large, a random subset of permutation $\mathcal{P}_0 \subset \mathcal{P}$ is employed.

Applying the previous formula to each interval leads to obtain an n dimensional vector $\boldsymbol{\varphi} = (\varphi_{\nu,1}, \dots, \varphi_{\nu,n})^T$. The *Shapley value function* is then the density function of the histogram-type measure defined by vector $\boldsymbol{\varphi}$:

$$\mathcal{R}_f(t) = \sum_{i=1}^n \frac{\varphi_{\nu,i}}{b_i - a_i} \mathbb{1}_{I_i}(t).$$

The Shapley value function can also be reported as the polygonal function which interpolates the points $((a_i + b_i)/2, \varphi_{\nu,i}/(b_i - a_i))$. Figure 2 shows an example of those functions. On the left side, a histogram-type function is depicted. On the right part, its equivalent polygonal function is shown. It should be noted that any of these functions has the following interpretation: the higher the value, the more relevant the interval is for the prediction model. Actually, $\varphi_{\nu,i}$ can be interpreted as the average increment of R^2 obtained when using $\mathcal{X}(t) \cdot \mathbb{1}_{I_i}(t)$ instead of its conditional expectation.

4.2 Feature selection based on infinite games

Our framework can be adapted to perform variable selection based on Shapley value, which requires the use of a continuous game. We propose to use two distinct games: the first one is inspired by the *minimum Redundancy*

Maximum Relevance method (mRMR; see Appendix A) while the second one is based on the *distance correlation* (see Appendix B).

Regarding mRMR method, let us consider Equation (3), which has the objective of computing the Shapley value for player i (or, equivalently, interval I_i). Recall that the elements of a given permutation π are intervals of the form I_k , $k \in N = \{1, \dots, n\}$ (Section 4.1). Furthermore, let \mathbf{X} be the $m \times T$ matrix representing the functional data set (Section 2.1). The set of points of I for which data have been observed and stored is $\mathcal{T} = \{t_1, \dots, t_T\}$.

Let p_π^i the players preceding player I_i in a given permutation π . Let $\mathcal{T}_{p_\pi^i} = \cup_{I_k \in p_\pi^i} (I_k \cap \mathcal{T})$ be the set of points that belong to \mathcal{T} and some interval of p_π^i . The *relevance* and *redundancy* of a non-empty set p_π^i is calculated according to Equation (4) and Equation (5) respectively (Appendix A) as

$$\text{Rel}(p_\pi^i) = \frac{1}{\text{card}(\mathcal{T}_{p_\pi^i})} \sum_{t \in \mathcal{T}_{p_\pi^i}} J(\mathbf{x}_t, \mathbf{y}),$$

$$\text{Red}(p_\pi^i) = \frac{1}{\text{card}^2(\mathcal{T}_{p_\pi^i})} \sum_{t_1, t_2 \in \mathcal{T}_{p_\pi^i}} J(\mathbf{x}_{t_1}, \mathbf{x}_{t_2}),$$

where \mathbf{y} is the m dimensional vector representing the target, \mathbf{x}_s corresponds to the s -th column of \mathbf{X} and J represents the absolute value of the Pearson correlation coefficient. In addition, when p_π^i is the empty set, $\text{Rel}(p_\pi^i) = 0$ and $\text{Red}(p_\pi^i) = 1$. Next, the game ν_Π is defined as $\nu_\Pi(p_\pi^i) = \text{Rel}(p_\pi^i)/\text{Red}(p_\pi^i)$. The same reasoning is applied to $p_\pi^i \cup I_i$, resulting in the computation of the Shapley value based on the mRMR method.

The distance correlation (see Appendix B) can also be considered as a means of accounting for variable selection in combination with the infinite games approach. Note that distance correlation involves the calculation of distance between functions. According to Equation (3), let π be a permutation and let p_π^i be the players preceding player I_i . The corresponding distance between functions \mathcal{X}_h and \mathcal{X}_ℓ is calculated as

$$d_{p_\pi^i}^2(\mathcal{X}_h, \mathcal{X}_\ell) = \|\mathcal{X}_h - \mathcal{X}_\ell\|_{p_\pi^i}^2 = \sum_{I_k \in p_\pi^i} \int_{I_k} [\mathcal{X}_h(t) - \mathcal{X}_\ell(t)]^2 dt.$$

The previous distance is computed for all pairs of functions in the test set. In practice, the trapezoidal rule is employed for numerical integration.

Following the notation of Appendix B, we define $a_{h\ell} = d_{p_\pi^i}^2(\mathcal{X}_h, \mathcal{X}_\ell)$ and $b_{h\ell} = |y_h - y_\ell|$, for $1 \leq h, \ell \leq m$. Then, using Equations (6) and (7) in Appendix B, the distance correlation is computed and denoted by $\hat{\mathcal{D}}(p_\pi^i, \mathbf{y})$. The role of the game ν_Π is assumed by the empirical distance correlation: $\nu_\Pi(p_\pi^i) = \hat{\mathcal{D}}(p_\pi^i, \mathbf{y})$.

As outlined in Section 4.1, instead of using the entire set of permutations \mathcal{P} when computing variable selection, a moderate random set of permutations is employed.

4.3 ShapleyFDA package

An open source Python package, `ShapleyFDA`, has been released to PyPI to compute the Shapley value function according to the methodology explained in this work. It contains functionalities for feature importance (Section 4.1) as well as for feature selection (Section 4.2). Given that the calculations are inherently matrix-intensive, the fundamental component of `ShapleyFDA` is based on the `NumPy` package (Harris et al. 2020).

As a large volume of computations must be considered, an efficient implementation has been conducted, whereby intermediate results are stored in memory for future reference. For instance, given permutations $\pi_1 = (I_3, I_4, I_1, I_2)$ and $\pi_2 = (I_3, I_4, I_2, I_1)$ the set of players preceding player 1 in π_1 is the same as the set of players preceding 2 in π_2 . Upon the initial computation of the value for $p_{\pi_1}^1 = \{I_3, I_4\}$, it is stored. This approach guarantees that the same value will not be calculated twice, but rather used as many times as is necessary.

`ShapleyFDA` assumes that the machine learning model has already been trained. Furthermore, the package is designed so that it can handle multiple prediction models simultaneously to obtain the Shapley value function for each of them, as well as for feature selection methods described in Section 4.2. Consequently, the same set of random permutations is used when obtaining multiple Shapley value functions. Moreover, the input test data set must be provided in the matrixwise formulation, as detailed in Section 2.1.

Finally, the package incorporates functionalities to display both figures, the histogram-type function and the polygonal-type function (Section 4.1). Apart from the released version in PyPI, it also has a development version, which is available at `GitHub`.

5 Experiments

Two types of experiments are conducted with the objective of showing the performance of our proposed methodology. In the first type, described in Section 5.1, we simulate data and then use three different machine learning models to predict the response variable. Since we control the data generation process, we know in advance which points are important. The second type, which is explained in Section 5.2, consists of exploring the Tecator data set (Borggaard and Thodberg 1992). The code utilised in the experimental configuration is accessible via `GitHub`, `github.com/pachoning/shapley_fda_experiments`. Simulated data are also available. Since their size is high and `GitHub` is not meant to store large volume of data, they are placed separately from the code at `https://bit.ly/4crYVt1`.

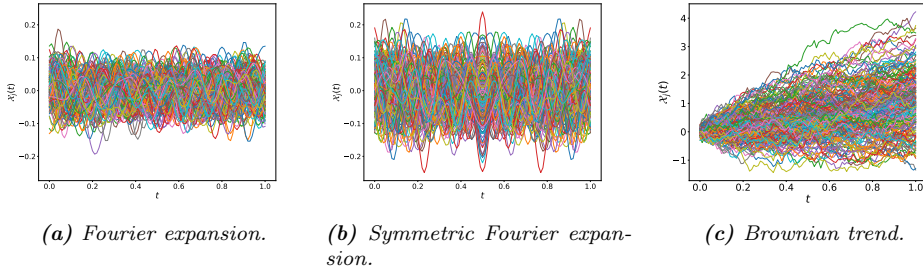


Figure 3: Functional data sets.

5.1 Simulated data

We begin by explaining how the pair of random variables (\mathcal{X}, Y) are obtained. Recall that our work just considers the scalar response on functional regressor (Section 2.1). In addition, the interval considered is the unitary one, i.e., $I = [0, 1]$. Regarding \mathcal{X} we consider 3 different ways of generation, namely *Fourier expansion*, *symmetric Fourier expansion* and *Brownian trend* (short name for *Brownian motion with a trend*). The first one consists of linear combinations of the Fourier basis,

$$\mathcal{X}_F(t) = \sum_{s=0}^r \mathcal{Z}_s \xi_s(t),$$

where \mathcal{Z}_s are independent draws of a standard normal distribution, $\{\xi_s(t)\}_{s \geq 0}$ is the Fourier basis on I , and r is an even number.

The goal of the second one is to obtain symmetric trajectories with respect to the middle point of I . This is achieved by building the functions as

$$\mathcal{X}_{\text{sF}}(t) = \mathcal{X}_F(t) + \mathcal{X}_F(1-t).$$

When simulating data for the previous two cases, $\mathcal{X}_F(t)$ and $\mathcal{X}_{\text{sF}}(t)$, the value of r is fixed to 30. The third functional random variable taken into account is a Brownian motion with a trend. Let $\mathcal{B}(t)$ be a Brownian motion for $t \in I$. Then, the functional random variable is

$$\mathcal{X}_B(t) = \mathcal{B}(t) + t.$$

Figure 3 illustrates the aforementioned functional random variables.

Every functional data set is stored in a matrix \mathbf{X} of size $m \times T$, where m takes 2 different values, 200 and 500, and T is equal to 101, being $t_1 = 0$ and $t_k = t_{k-1} + 0.01$, $k = 2, \dots, 101$. Regarding the partition $\mathcal{I} = \{I_1, \dots, I_n\}$, we consider $n = 20$ and all the intervals with the same length.

In order to build the target variable Y , a transformation is applied to the functional random variable, $\Upsilon : L^2(I) \rightarrow \mathbb{R}$, leading to $Y = \Upsilon(\mathcal{X}) + \epsilon$,

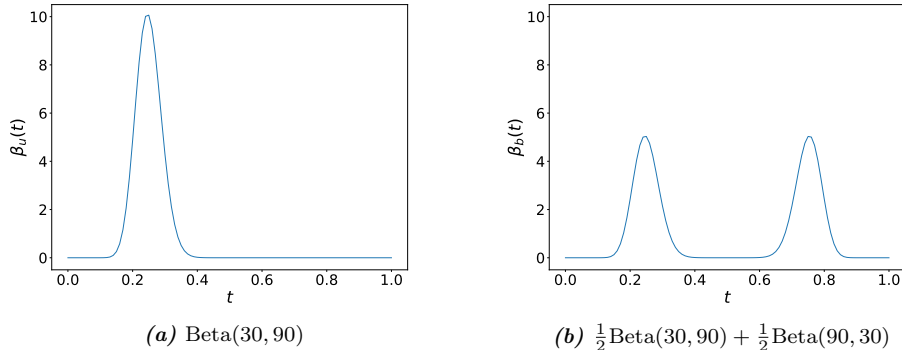


Figure 4: Beta density functions.

being $\epsilon \sim N(0, \sigma_\epsilon^2)$ and independent of \mathcal{X} . We control the signal-to-noise ratio by using $\eta = \sigma_\epsilon^2 / \sigma_Y^2$, where $\sigma_Y^2 = \text{Var}(Y)$. We use two values for η : 0.05 and 0.25. With respect to Υ , 4 types of transformations are taken into account:

- *Linear unimodal*, $\Upsilon_{\text{lu}}(\mathcal{X}) = \int_I \mathcal{X}(t) \beta_{\text{u}}(t) dt$, with $\beta_{\text{u}}(t)$ being the density function of a Beta distribution with parameters 30 and 90. Left part of Figure 4 depicts this function.
- *Linear bimodal*, $\Upsilon_{\text{lb}}(\mathcal{X}) = \int_I \mathcal{X}(t) \beta_{\text{b}}(t) dt$, with $\beta_{\text{b}}(t) = (1/2)[\beta_{\text{u}}(t) + \beta_{\text{u}}(1-t)]$. Right part of Figure 4 shows this function.
- *Non-linear*, $\Upsilon_{\text{nl}}(\mathcal{X}) = \max_{t \in I} \{|\beta_{\text{u}}(t) \mathcal{X}(t)|, |\beta_{\text{u}}(t) \mathcal{X}(1-t)|\}$.
- *Discrete*, $\Upsilon_{\text{d}}(\mathcal{X}) = \mathcal{X}(0.15) + |\mathcal{X}(0.55)| + \mathcal{X}^2(0.35) \mathcal{X}(0.85)$.

In total, there are 48 different scenarios to simulate, the result of combining all the possibilities:

$$\{\mathcal{X}_{\text{F}}(t), \mathcal{X}_{\text{sF}}(t), \mathcal{X}_{\text{B}}(t)\} \times \underbrace{\{200, 500\}}_m \times \underbrace{\{0.05, 0.25\}}_\eta \times \{\Upsilon_{\text{lu}}, \Upsilon_{\text{lb}}, \Upsilon_{\text{nl}}, \Upsilon_{\text{d}}\}.$$

The relationship between \mathcal{X} and Y is modelled using three distinct machine learning algorithms: a functional linear regression model (FLM for short and explained in Section 2.1), a functional K-Nearest Neighbour algorithm (FKNN for short; Ferraty and Vieu 2006) and a functional version of neural networks (FNN for short; Heinrichs et al. 2023). As for the software used to train those models, `scikit-fda` (Ramos-Carreño et al. 2024) contains an implementation of FLM and FKNN. In addition, Florian Heinrichs has an open source implementation of FNN available at [GitHub \(github.com/FlorianHeinrichs/functional_neural_networks\)](https://github.com/FlorianHeinrichs/functional_neural_networks).

A scenario is *replicated* 100 times. A replica is constituted by the generation of three independent data sets: training, validation and test. The

first one is used to train the machine learning models. As those algorithms require hyperparameter tuning, the second data set is used to do it. Finally, the goal of the third data set is to compute the Shapley value function for each machine learning algorithm. These 3 sets are of the same shape, $m \times T$. So, given a scenario, there are 100 sets of Shapley value functions. A total of $|\mathcal{P}_0| = 1000$ uniformly random permutations of the set \mathcal{I} are generated.

Apart from the Shapley value function for each of the 3 machine learning algorithms (Section 4.1), we also provide 2 additional Shapley value functions: one using the mRMR principle with Pearson correlation coefficient, and another using the distance correlation (Section 4.2). Therefore, 5 Shapley value functions are obtained for each scenario and each of its 100 simulations. We show the mean function for each of the 5 Shapley value functions and each scenario, averaged over the 100 simulations.

Prior to the presentation of the results, we describe two adjustments performed. Firstly, instead of using the distance correlation as the game, it is considered its square, i.e., \mathcal{D}^2 (Appendix B). Since the measure employed for machine learning models is the (squared) coefficient of determination, for the sake of homogeneity, we consider to use the square for the distance correlation.

Secondly, as the scale of the mRMR Shapley value function may vary considerably in comparison to the other functions, each mRMR Shapley value function is rescaled in order to ensure that its range is aligned with that of the other functions. Precisely, for $t \in I$ let $\mathcal{R}_{\text{mRMR}}(t)$ be the mRMR Shapley value function and let $\mathcal{R}_j(t)$, $j = 1, \dots, 4$, be the other 4 Shapley value functions. Then, the mRMR Shapley value function considered is $(\kappa_2/\kappa_1)\mathcal{R}_{\text{mRMR}}(t)$, where $\kappa_1 = \max_t \mathcal{R}_{\text{mRMR}}(t)$ and $\kappa_2 = \max_{j,t} \{\mathcal{R}_j(t)\}$. These two adjustments are performed individually in each of the 100 replicas before computing the mean function.

For the sake of brevity, we offer here the results corresponding to sample size 200 and signal-to-noise ratio given by $\eta = 0.025$ (12 scenarios out of 48; the remaining results are reported in Appendix D). Figure 5 shows the Shapley value functions, and Table 1 contains the mean and the standard deviation (in brackets) across the 100 simulations of $R^2(I)$, that is the coefficient of determination using all points $t \in [0, 1]$ evaluated on the test data sets.

First, we consider the scenarios with functional data generated as Fourier expansions (first column in Figure 5). When the target variable is derived from the linear unimodal or bimodal transformations (first and second row respectively), all the Shapley value functions are able to identify the area with the highest relevance, which is the one formed by the points where the functional coefficients ($\beta_u(t)$ or $\beta_b(t)$) take their maximum values. Regarding the coefficients of determination $R^2(I)$, they indicate good fitting for both, FLM and FNN, and a poor performance of FKNN.

The third scenario (first column, third row in Figure 5), with target of

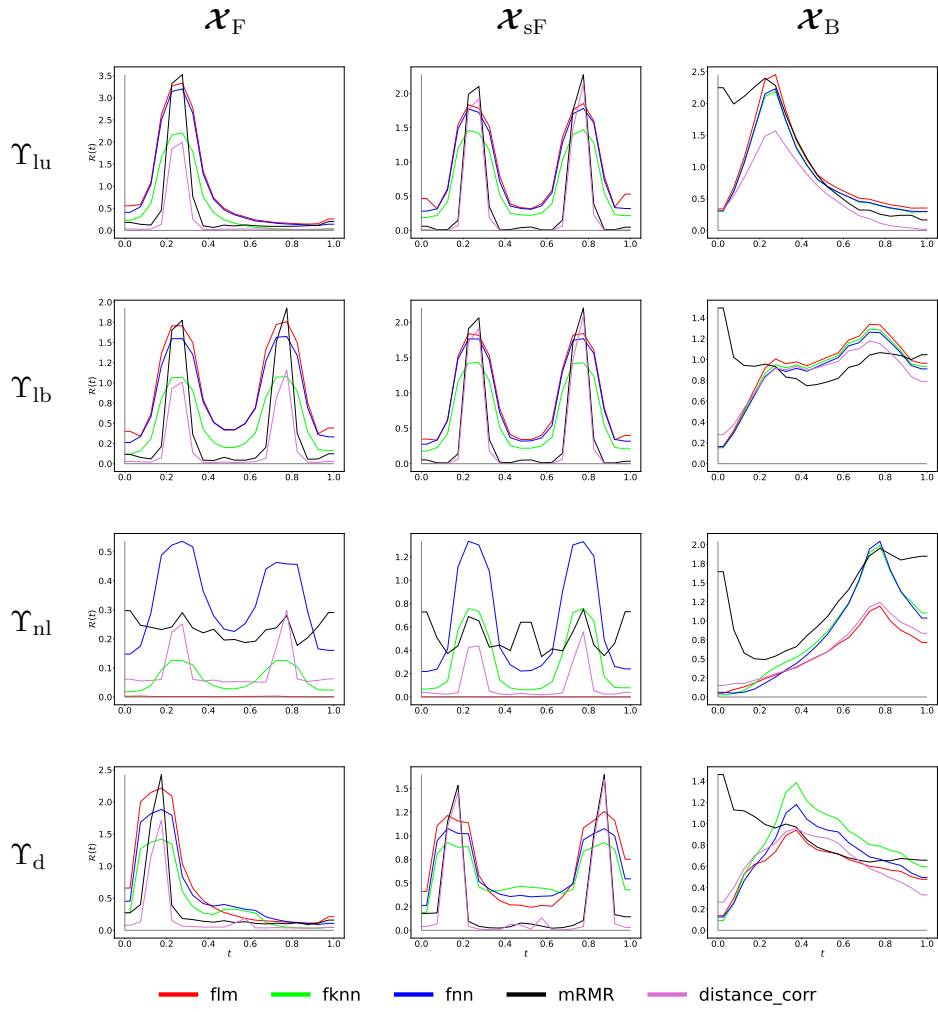


Figure 5: Mean Shapley value functions for those scenarios with $m = 200$ and $\eta = 0.05$.

Table 1: Mean value (standard deviation) of $R^2(I)$ of FLM, FKNN and FNN for those scenarios with $m = 200$ and $\eta = 0.05$.

		\mathcal{X}_F	\mathcal{X}_{sF}	\mathcal{X}_B
Υ_{lu}	FLM	0.9468 (0.0054)	0.9483 (0.0053)	0.9467 (0.0058)
	FKNN	0.5399 (0.0392)	0.7048 (0.0259)	0.8541 (0.0191)
	FNN	0.8887 (0.0812)	0.8961 (0.0902)	0.8602 (0.1160)
Υ_{lb}	FLM	0.9464 (0.0062)	0.9470 (0.0053)	0.9479 (0.0051)
	FKNN	0.5377 (0.0370)	0.6962 (0.0273)	0.9149 (0.0091)
	FNN	0.8634 (0.0726)	0.9053 (0.0719)	0.8924 (0.0521)
Υ_{nl}	FLM	0.0289 (0.0331)	0.0264 (0.0326)	0.5718 (0.0753)
	FKNN	0.0490 (0.0804)	0.3101 (0.0668)	0.8637 (0.0163)
	FNN	0.3361 (0.1450)	0.6559 (0.1602)	0.8321 (0.0721)
Υ_d	FLM	0.6696 (0.0388)	0.6907 (0.0383)	0.6209 (0.0462)
	FKNN	0.4337 (0.0397)	0.5990 (0.0372)	0.8324 (0.0464)
	FNN	0.6070 (0.1568)	0.6492 (0.0909)	0.7196 (0.0644)

non-linear type, shows that the Shapley value functions may be different from each other. First, it can be seen that the Shapley value function corresponding to the functional linear model is constantly equal to 0. According to it, no point is relevant for the model. As the relationship between \mathcal{X} and Y is non-linear, the estimated FLM is of very poor quality. This can be corroborated with the value of its $R^2(I)$, which mean value is close to 0 (see Table 1). Therefore, it is expected not to find any relevant point $t \in I$ when using the FLM. However, FKNN and FNN models are able to detect the relevant points in prediction, with FNN showing a better performance than FKNN.

Regarding the Shapley value functions based on feature selection, on the one hand, the distance correlation is in the same line as FKNN and FNN, with an intermediate behaviour. On the other hand, the mRMR Shapley value function is approximately constant because it is based on pointwise linear correlations and therefore, it is not able to capture the non-linear relationships present in this scenario (recall that the scale of this function is arbitrarily chosen for graphical visibility). Consequently, the mRMR Shapley value function behaves similarly to that of FLM.

Consider now the fourth set of Shapley value functions in the first column of Figure 5. It corresponds to using a discrete transformation when defining the target variable, $\Upsilon_d(\mathcal{X}) = \mathcal{X}(0.15) + |\mathcal{X}(0.55)| + \mathcal{X}^2(0.35)\mathcal{X}(0.85)$, which depends only on the values of \mathcal{X} at four points (0.15, 0.35, 0.55 and 0.85). The 5 Shapley value functions indicate that the most relevant points t are those around 0.15, and that small to no relevance is assigned to the points 0.35, 0.55 or 0.85.

Since the values taken by \mathcal{X} are close to 0, the result of $\mathcal{X}^2(0.35)\mathcal{X}(0.85)$ is a very small number. So, its effect over $\Upsilon_d(\mathcal{X})$ is expected to be negligible. As can be observed in the aforementioned figure, the values around $t \in \{0.35, 0.85\}$ have almost no impact, although there is a local maximum at $t = 0.85$. Regarding $t = 0.55$, as the absolute value is applied to $\mathcal{X}(0.55)$, the degree of variability of $\mathcal{X}(0.55)$ is limited to half. Therefore, the relevance of the point $t = 0.55$ is expected to be low. These conclusions are supported by the Shapley value functions depicted in the aforementioned figure.

The second column of Figure 5 corresponds to the scenarios where data are generated using the symmetric Fourier expansion. The same insights derived for the first column can be applied in these 4 scenarios, with the exception that, as symmetric functions are employed, in all cases two relevant areas are obtained, which are symmetric with respect to the midpoint $t = 0.5$.

Finally, let us consider the last column of Figure 5, which corresponds to scenarios whose data are generated using a Brownian motion with a trend. The first row corresponds to a linear unimodal transformation. All Shapley value functions consider the most relevant point to be the one that maximises $\beta_u(t)$. In the case of the scenario where a linear bimodal is used (second row), two areas are particularly relevant in this regard: the first corresponds with points close to $t_1 = 0.25$ and the second with points close to $t_2 = 0.75$, being $\{t_1, t_2\} = \operatorname{argmax}_{t \in I} \beta_b(t)$. As the variance of the Brownian trend increases with t , there is more variability for points close to $t = 0.75$ than for points close to $t = 0.25$, and therefore, it is expected to obtain a higher relevance in the neighbourhood of t_2 , a phenomenon that is indeed observed.

A similar line of reasoning explains why the highest relevance of the non-linear transformation (third row) is around $t = 0.75$: as the variance increases with t , $\max_{t \in I} \{|\beta_u(t)\mathcal{X}(t)|, |\beta_u(t)\mathcal{X}(1-t)|\}$ is around $t = 0.75$ instead of $t = 0.25$. With regard to the discrete transformation (fourth row), the most relevant point is $t = 0.35$, which is explained by (1) now the range of variability of $\mathcal{X}^2(0.35)\mathcal{X}(0.85)$ is larger than that of $\mathcal{X}(0.15)$ and $|\mathcal{X}(0.55)|$ (see Figure 6, corresponding to the Brownian trend data set shown in the rightmost part of Figure 3) and (2) $\mathcal{X}(0.35)$ is more difficult to predict than $\mathcal{X}(0.85)$ using conditional expectations, because $t = 0.85$ is closer to the end of the path $\{\mathcal{X}(t) : t \in [0, 1]\}$ than $t = 0.35$.

The only Shapley value function that shows a slightly different behaviour across all the scenarios of the last column of Figure 5 is the mRMR Shapley value function. According to it, the beginning of the interval I can be considered relevant, contrary to what the other 4 functions show. One possible explanation for this phenomenon is that the redundancy for the initial intervals is relatively low in comparison to that of the subsequent intervals, as illustrated in Figure 7, and redundancy appears in the denominator of mRMR measure.

A final remark on the computational times is in order. The main compu-

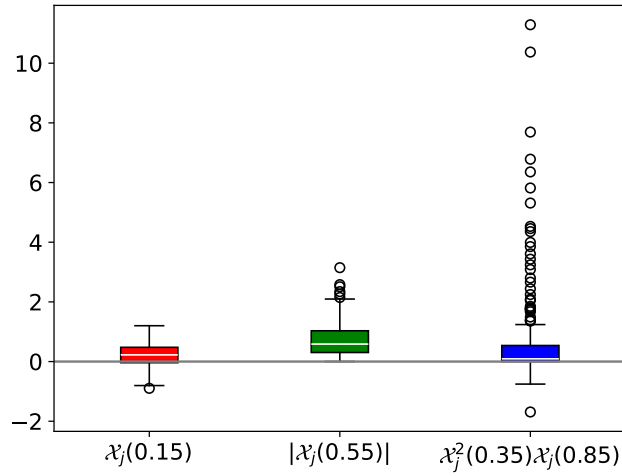


Figure 6: Left: boxplot of $\{\mathcal{X}_j(0.15)\}_{j=1}^m$. Middle: boxplot of $\{|\mathcal{X}_j(0.55)|\}_{j=1}^m$. Right: boxplot of $\{\mathcal{X}_j^2(0.35)\mathcal{X}_j(0.85)\}_{j=1}^m$ where, $\{\mathcal{X}_j\}_{j=1}^m$ corresponds to the Brownian trend data set shown in the rightmost part of Figure 3.

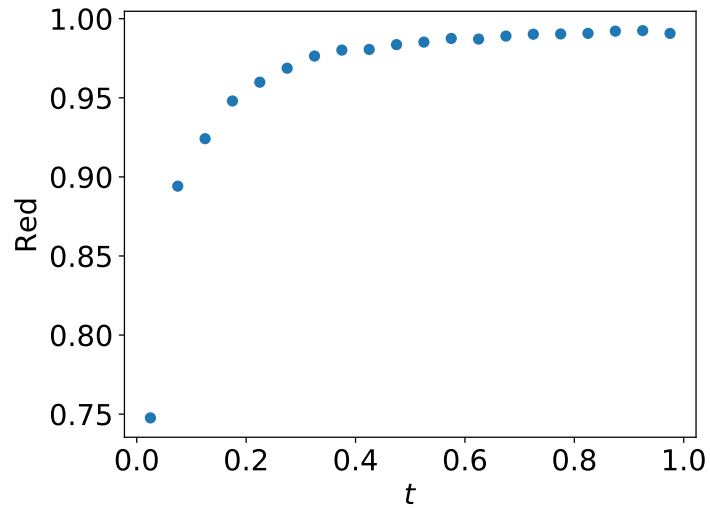


Figure 7: Redundancy for the Brownian trend data set shown in the rightmost part of Figure 3.

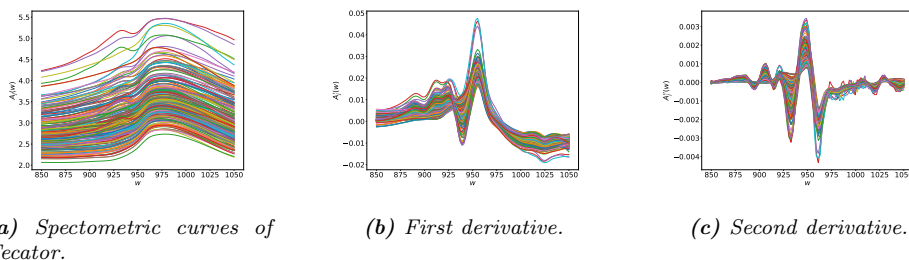


Figure 8: Tecator data set.

tational burden of the algorithm is the large number of random permutations required in order to approximate the Shapley values. For instance, a single simulation of those employed to generate the graphic of first row and first column of Figure 5 (which uses 1000 random permutations) takes 1005 seconds to compute the FLM Shapley value function in a virtual machine with 16vCPU (8 core) with 16GB of RAM. To evaluate the effect of the number of random permutations, we repeat this experiment with 2000 and 5000 random permutations, resulting in computation times 1854 and 4210 seconds respectively. As can be observed, one of the main drawbacks of our proposal is its high computational cost. The bottleneck of this algorithm is placed in the conditional expectation, since it must be calculated for each of the functions of the data set.

5.2 Real data

Tecator data set has been widely used within the FDA literature (see, for instance, Ferraty and Vieu 2006). This data set consists of 215 spectrometric curves of meat samples and it measures the near infrared (NIR) absorbance $A(w)$ as a function of wavelength w (in nanometres). In addition, each curve is associated with three distinct quantities: the percentage of fat, water, and protein in the meat sample. The percentage of fat is used here as the target variable. Figure 8 depicts the set of spectrometric curves (left), their first derivatives (middle) and their second derivatives (right).

Following Ferraty and Vieu (2006, Section 7.2.1), we divide the data set into *learning sample* (curves 1 to 160; 74.4%) and *testing sample* (curves 161 to 215; 55 curves, 25.6%). Given that we differentiate between *training* and *validation* sets, we divide the learning sample randomly into *training set* (128 curves; 59.6%) and *validation set* (32 curves; 14.8%). The training set is employed for fitting the same machine learning algorithms used in Section 4.1: FLM, FKNN and FNN. The validation set is used to perform hyperparameter tuning, and the test data set serves to compute the distinct Shapley value functions.

The prediction algorithms are used to model the target variable as a

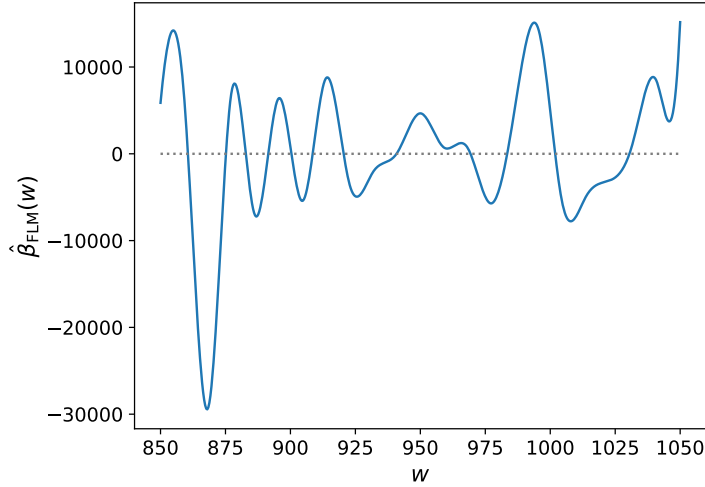


Figure 9: Estimated beta function for the functional linear model using Tecator data set to predict the fat content.

function of the second derivatives of the spectrometric curves, as suggested by Ferraty and Vieu (2006, Section 7.2.2). See also Boj, Delicado, and Fortiana (2010). Regarding the functional neural network, we employ the same architecture as Heinrichs et al. (2023). The coefficients of determination, $R^2(I)$, are 0.962 for FLM, 0.9808 for FKNN and 0.8196 for FNN. Regarding FLM, Figure 9 shows the estimated function $\hat{\beta}(t)$. As it can be seen, this function is highly fluctuating and difficult to interpret.

Next, we use our proposal to obtain interpretability for each of the machine learning models, as in Section 5.1. The interval of interest, $I = [850, 1050]$, is divided into 20 parts, all of the same length, and 5000 permutations are performed.

Figure 10 depicts the Shapley value functions (up), aligned with the set of second derivatives (middle) and their mean function (down). It should be recalled that the relevance is obtained at interval level, the most relevant of which are coloured in the uppermost part of Figure 10. On the other hand, in the middle and the lowest part of that figure we highlight the point that we consider to be important within each relevant interval.

All the Shapley value functions coincide that the interval $[1000, 1010]$ (depicted in purple in Figure 10) is relevant (at least locally). According to the mRMR Shapley value function, this is the most relevant interval. The mean function shows a local maximum at $w = 1005$. There are 3 intervals considered relevant by the machine learning models: $[1040, 1050]$, $[950, 960)$ and $[930, 940)$, in brown, red and green respectively in Figure 10. According to FLM and FKNN, $[1040, 1050]$ is the most relevant interval. In addition, the distance correlation Shapley value function also considers it an important interval. It is the last interval of the partition and the data set

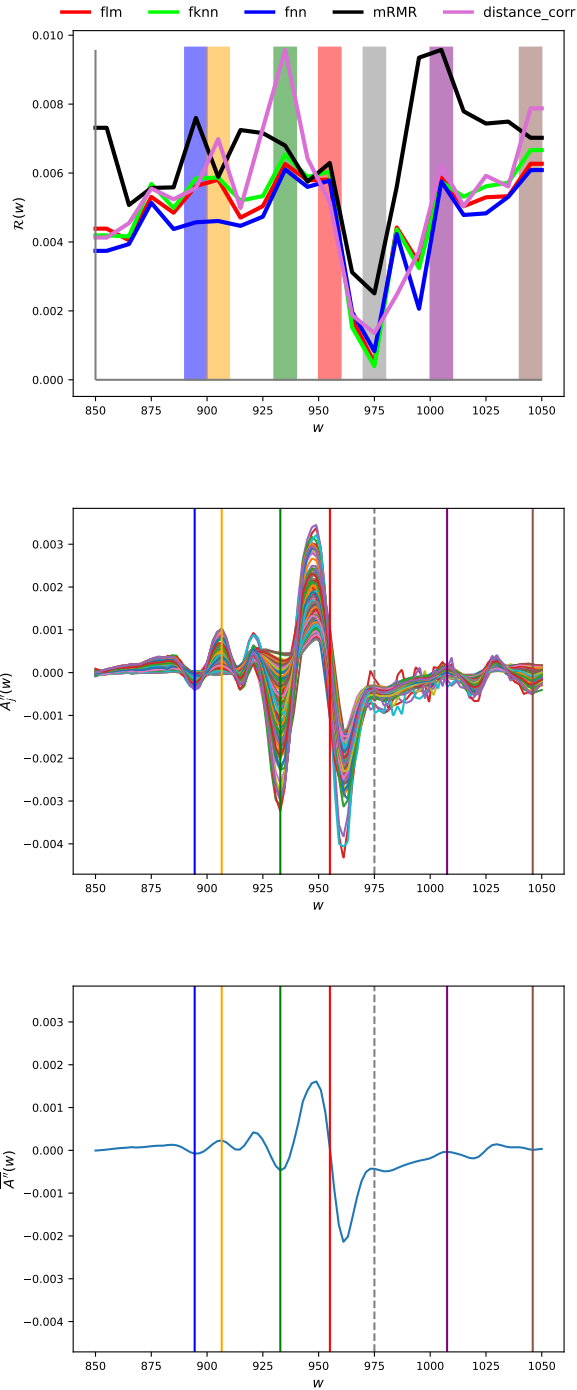


Figure 10: Up: Shapley value functions for Tecator data set. Vertical coloured bars indicate the most relevant intervals. Middle: set of second derivatives. Down: mean function of the second derivatives.

containing the second derivative exhibits some degree of variability, while the mean function indicates a local minimum at $w = 1045$.

Regarding $[950, 960)$, the mRMR Shapley value function also identifies it as a relevant interval. This interval is situated between the global minimum and the global maximum of the mean function of the second derivatives, both located at $w = 949$ and $w = 961$ respectively. As for the interval $[930, 940)$, it is the most relevant interval according to the distance correlation Shapley value function as well as to the FNN Shapley value function. Note that there is a local minimum inside it, at $w = 936$, for the mean function of the second derivatives.

It is of interest to note the existence of two additional relevant intervals, $[900, 910)$ and $[890, 900)$, in orange and blue in Figure 10. As for $[900, 910)$ concerns, the Shapley value functions of FLM, FKNN and distance correlation consider it as locally relevant. Inside this interval, the mean of second derivatives has a local maximum at $w = 906$. On the other hand, regarding the interval $[890, 900)$, it is considered locally important according to FLM, FKNN and mRMR Shapley value functions. Inside this interval, concretely at $w = 894$, there is a local minimum of the mean of second derivatives.

It is also noteworthy that all Shapley value functions identify the interval $[970, 980)$ as the least relevant. This is likely due to the fact that the values of all second derivatives are in close proximity at this interval (see the dashed lines in Figure 10 at $w = 975$).

6 Conclusions

In light of the considerable extent of the presence of Artificial Intelligence in our society, it is of particular importance to gain insight into the mechanisms through which it learns. This work represents a novel approach to addressing the global interpretability of prediction models within the field of Functional Data Analysis.

Our framework is based on Game Theory for games with a continuum of players, extending the Shapley value to the case of a set of infinite regressors. The central piece of this work is the Shapley value function, that measures the relevance of all points of the interval where the functional data are observed. In addition, we enrich this methodology with tools from feature selection. Alongside this manuscript, we present an open source `Python` package that implements this framework.

We have illustrated the performance of our work by means of a set of experiments. On the one hand, we use simulated data where the relevant points were known beforehand. The results have shown that these points have been successfully captured by the explainability method. On the other hand, we have explored the Tecator data set, where the second derivative has been used to model the data. According to our proposal, the most

relevant intervals contains local extremes of the mean function of the second derivatives.

As future research, the high computational cost must be addressed. In addition, it would be interesting to extend this methodology in two directions: first, considering several functional regressors, and second, allowing a functional response and regressors that are either scalar or functional.

A Minimum Redundancy Maximum Relevance

Ding and Peng (2005) present *minimum Redundancy Maximum Relevance* (mRMR for short), a framework to perform variable selection in prediction problems with a finite number of predictors, where they look for a reasonable trade-off between *relevance* and *redundancy*.

Let (\mathcal{W}, Y) , $\mathcal{W} \in \mathbb{R}^p$, $Y \in \mathbb{R}$ a pair of random variables. First, an *association metric* J for pairs of variables is defined. The original work uses the *mutual information* metric, but any other can be used: Pearson correlation, Spearman rank correlation, etc. Afterwards, they propose to measure both relevance and redundancy respectively as:

$$\text{Rel}(F) = \frac{1}{\text{card}(F)} \sum_{t \in F} J(\mathcal{W}_t, Y), \quad (4)$$

$$\text{Red}(F) = \frac{1}{\text{card}^2(F)} \sum_{s, t \in F} J(\mathcal{W}_t, \mathcal{W}_s), \quad (5)$$

where $F \subset \{1, \dots, p\}$ and $\text{card}(F)$ means the cardinal of F . The mRMR algorithm aims at maximising the relevance while maintaining a minimal level of redundancy. To obtain an appropriate set of relevant features, the algorithm employs the following strategy:

1. Select the variable that maximises $\text{Rel}(F)$ among all sets of the type $F_i = \{i\}$, $i \in \{1, \dots, p\}$.
2. Then, the variables should be added to the set F in a sequential manner, with the goal of maximising $\text{Rel}(F) - \text{Red}(F)$ or $\text{Rel}(F)/\text{Red}(F)$.
3. Finally, stop when a certain criteria is reached.

An exhaustive comparative study based on mRMR variable selection for functional data is done in Berrendero, Cuevas, and Torrecilla (2016). The authors consider a *functional explanatory variable* $\mathcal{X}(t)$ and its discrete representation, a vector of length T , to carry out such a study. Taking into account the previous notation for mRMR, $p = T$, $\mathcal{W}_1 = \mathcal{X}(t_1), \dots, \mathcal{W}_T = \mathcal{X}(t_T)$ and $F \subset \{t_1, \dots, t_T\}$. Let us remark that in this manuscript we only use Equations (4) and (5), without going through steps 1, 2 and 3.

B Distance correlation

The *distance correlation* (Székely, Rizzo, and Bakirov 2007) is a measure of dependence between two random vectors $\mathcal{S}_1, \mathcal{S}_2$, where $\mathcal{S}_1 \in \mathbb{R}^p$ and $\mathcal{S}_2 \in \mathbb{R}^q$. Let ϕ, ϕ_1 and ϕ_2 be the characteristic function of $(\mathcal{S}_1, \mathcal{S}_2), \mathcal{S}_1$ and \mathcal{S}_2 respectively. The *distance covariance* is defined as the positive square root of

$$\mathcal{V}^2(\mathcal{S}_1, \mathcal{S}_2) = \int_{\mathbb{R}^{p+q}} |\phi(u, v) - \phi_1(u)\phi_2(v)|^2 w(u, v) dudv,$$

with $w(u, v) = (c_p c_q \|u\|_p^{1+p} \|v\|_q^{1+q})^{-1}$, where $c_r = \frac{\pi^{(1+r)/2}}{\Gamma((1+r)/2)}$ is half the surface area of the unit sphere in \mathbb{R}^{r+1} and $\|\cdot\|_r$ is the Euclidean norm in \mathbb{R}^r . The distance correlation is the standardised version of the distance covariance: it is defined as the positive square root of

$$\mathcal{D}^2(\mathcal{S}_1, \mathcal{S}_2) = \frac{\mathcal{V}^2(\mathcal{S}_1, \mathcal{S}_2)}{\sqrt{\mathcal{V}^2(\mathcal{S}_1, \mathcal{S}_1)\mathcal{V}^2(\mathcal{S}_2, \mathcal{S}_2)}}.$$

It is of particular importance to emphasise that distance correlation characterises independence: \mathcal{S}_1 and \mathcal{S}_2 are independent if and only if $\mathcal{D}^2(\mathcal{S}_1, \mathcal{S}_2) = 0$. It is also noteworthy that the dimensions of the spaces in which both random vectors are situated are not required to be equal.

In the original paper, the authors proposed an estimator based on distances. Let $(\mathcal{S}_{11}, \mathcal{S}_{21}) \dots, (\mathcal{S}_{1m}, \mathcal{S}_{2m})$ be a sample of $(\mathcal{S}_1, \mathcal{S}_2)$. The double centring matrix of distances is computed as

$$A_{h\ell} = a_{h\ell} - \bar{a}_{h.} - \bar{a}_{. \ell} + \bar{a}_{..},$$

with elements $a_{h\ell} = \|\mathcal{S}_{1h} - \mathcal{S}_{1\ell}\|_p$, $\bar{a}_{h.} = 1/m \sum_{\ell=1}^m a_{h\ell}$, $\bar{a}_{. \ell} = 1/m \sum_{h=1}^m a_{h\ell}$ and $\bar{a}_{..} = 1/m^2 \sum_{h, \ell=1}^m a_{h\ell}$ where $h, \ell \in \{1, \dots, m\}$. Similarly is defined $B_{h\ell}$ using the sample of \mathcal{S}_2 . The empirical (square) distance covariance is defined as

$$\hat{\mathcal{V}}^2(\mathcal{S}_1, \mathcal{S}_2) = \frac{1}{m^2} \sum_{h, \ell=1}^m A_{h\ell} B_{h\ell}. \quad (6)$$

The empirical (square) distance correlation is computed by means of standardising the empirical distance covariance:

$$\hat{\mathcal{D}}^2(\mathcal{S}_1, \mathcal{S}_2) = \frac{\hat{\mathcal{V}}^2(\mathcal{S}_1, \mathcal{S}_2)}{\sqrt{\hat{\mathcal{V}}^2(\mathcal{S}_1, \mathcal{S}_1)\hat{\mathcal{V}}^2(\mathcal{S}_2, \mathcal{S}_2)}}. \quad (7)$$

C Estimating conditional expectations in a Gaussian process

In this section we describe how $\hat{\mathcal{X}}_j(t) = \mathbb{E}(\mathcal{X}(t) \mid \{\mathcal{X}(u) = \mathcal{X}_j(u) : u \in S\})$ is estimated, $1 \leq j \leq m$. We maintain the same notation as in the main

part of this manuscript. As mentioned in Section 4.1, it is assumed that \mathcal{X} is a Gaussian process observed at the set of points $\mathcal{T} = \{t_1, \dots, t_T\}$. Then, $(\mathcal{X}(t_1), \dots, \mathcal{X}(t_T))$ follows a multivariate normal distribution (with mean $\boldsymbol{\mu}$ and variance matrix $\boldsymbol{\Sigma}$) from which there are m independent observations. Let \mathbf{X} be the resulting $m \times T$ data matrix.

Let I_i , π and p_π^i be an interval (a player), a permutation and the set of players preceding i in π , respectively. Let $\mathcal{T}_{p_\pi^i} = \cup_{I_k \in p_\pi^i} (I_k \cap \mathcal{T})$ be the set of points that belong to \mathcal{T} and some interval of p_π^i , and let $\mathcal{J}_{p_\pi^i}$ be the corresponding indexes in $\{1, \dots, T\}$. We refer to $\mathcal{J}_{p_\pi^i}^c$ as the complementary set of $\mathcal{J}_{p_\pi^i}$. For the sake of clarity, we use the labels “1” for the set $\mathcal{J}_{p_\pi^i}^c$ and “2” for the set $\mathcal{J}_{p_\pi^i}$. The estimated variance covariance matrix from \mathbf{X} , $\hat{\boldsymbol{\Sigma}}$, can be rearrange as

$$\hat{\boldsymbol{\Sigma}} = \begin{bmatrix} \hat{\boldsymbol{\Sigma}}_{11} & \hat{\boldsymbol{\Sigma}}_{12} \\ \hat{\boldsymbol{\Sigma}}_{21} & \hat{\boldsymbol{\Sigma}}_{22} \end{bmatrix}.$$

Let $\hat{\boldsymbol{\mu}}_1$ be the estimation of the mean vector for those column whose indexes belong to $\mathcal{J}_{p_\pi^i}^c$. Likewise, let $\hat{\boldsymbol{\mu}}_2$ be the estimated mean vector for $\mathcal{J}_{p_\pi^i}$. Let \mathbf{x}_{j2} be the vector that results from selecting the j -th row of \mathbf{X} and those columns whose indexes belong to $\mathcal{J}_{p_\pi^i}$. Therefore, the standard theory of multivariate normal distributions states that

$$\begin{aligned} \{\hat{\mathcal{X}}_j(t_h) : h \in \mathcal{J}_{p_\pi^i}^c\} &= \hat{\mathbb{E}}(\{\mathcal{X}(t_h) : h \in \mathcal{J}_{p_\pi^i}^c\} \mid \{\mathcal{X}(t_o) = \mathcal{X}_j(t_o) : o \in \mathcal{J}_{p_\pi^i}\}) = \\ &\hat{\boldsymbol{\mu}}_1 + \hat{\boldsymbol{\Sigma}}_{12} \hat{\boldsymbol{\Sigma}}_{22}^{-1} (\mathbf{x}_{j2} - \hat{\boldsymbol{\mu}}_2). \end{aligned}$$

D Results of simulation study

In this section we present the results of the remaining scenarios, which are:

- $m = 200$ and $\eta = 0.25$. See Figure 11 and Table 2.
- $m = 500$ and $\eta = 0.05$. See Figure 12 and Table 3.
- $m = 500$ and $\eta = 0.25$. See Figure 13 and Table 4.

Acknowledgments

This research was supported by the Spanish Research Agency (AEI) under project PID2023-148158OB-I00, by AGAUR under the grant 2020 FI SDUR 306 and by UPC under AGRUPS-2024.

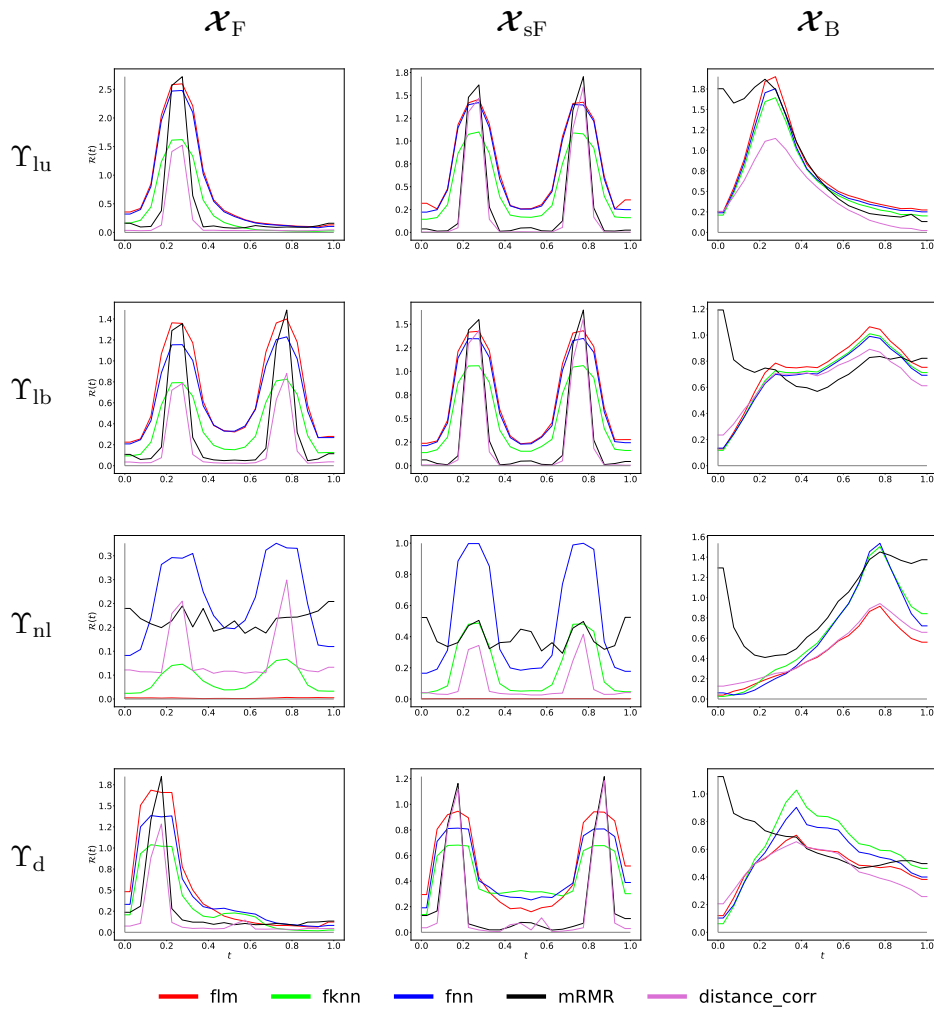


Figure 11: Mean Shapley value functions for those scenarios with $m = 200$ and $\eta = 0.25$.

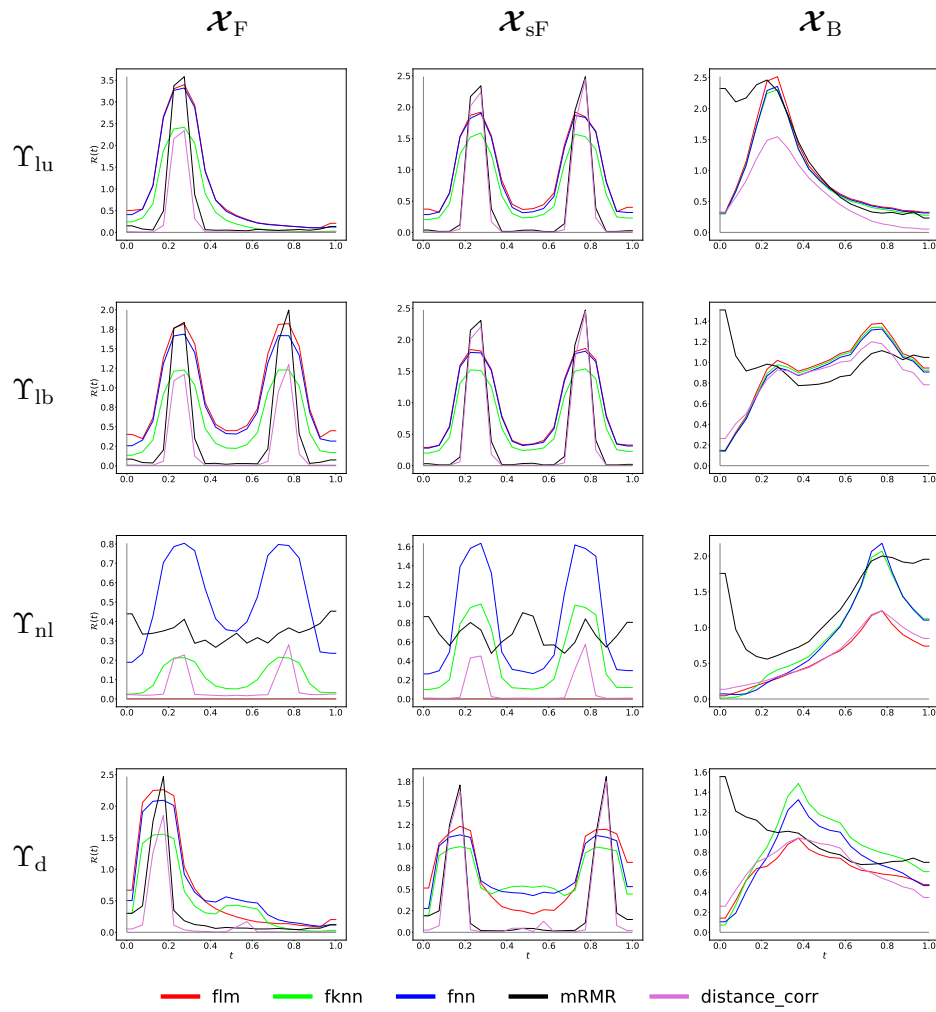


Figure 12: Mean Shapley value functions for those scenarios with $m = 500$ and $\eta = 0.05$.

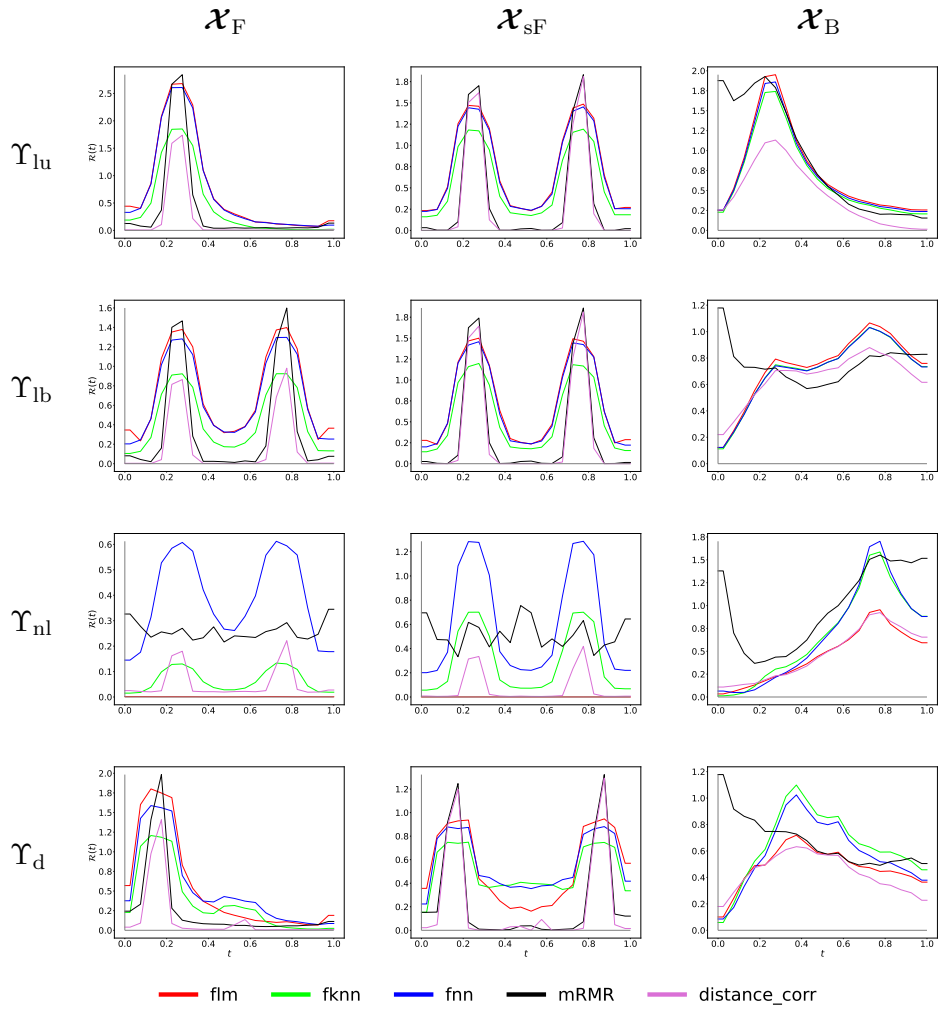


Figure 13: Mean Shapley value functions for those scenarios with $m = 500$ and $\eta = 0.25$.

Table 2: Mean value (standard deviation) of $R^2(I)$ of FLM, FKNN and FNN for those scenarios with $m = 200$ and $\eta = 0.25$.

		\mathcal{X}_F	\mathcal{X}_{sF}	\mathcal{X}_B
Υ_{lu}	FLM	0.7317 (0.0282)	0.7399 (0.0260)	0.7384 (0.0227)
	FKNN	0.3987 (0.0412)	0.5235 (0.0415)	0.6429 (0.0322)
	FNN	0.6936 (0.0570)	0.7137 (0.0418)	0.6884 (0.0655)
Υ_{lb}	FLM	0.7315 (0.0278)	0.7358 (0.0303)	0.7441 (0.0257)
	FKNN	0.3995 (0.0398)	0.5192 (0.0355)	0.7061 (0.0280)
	FNN	0.6542 (0.0720)	0.6945 (0.0683)	0.6919 (0.0586)
Υ_{nl}	FLM	0.0271 (0.0285)	0.0206 (0.0225)	0.4460 (0.0798)
	FKNN	0.0184 (0.0692)	0.2036 (0.0551)	0.6566 (0.0342)
	FNN	0.2147 (0.0952)	0.5086 (0.1176)	0.6271 (0.0864)
Υ_d	FLM	0.5010 (0.0556)	0.5248 (0.0488)	0.4911 (0.0490)
	FKNN	0.3161 (0.0513)	0.4414 (0.0395)	0.6274 (0.0530)
	FNN	0.4504 (0.1057)	0.4973 (0.0821)	0.5677 (0.0618)

Table 3: Mean value (standard deviation) of $R^2(I)$ of FLM, FKNN and FNN for those scenarios with $m = 500$ and $\eta = 0.05$.

		\mathcal{X}_F	\mathcal{X}_{sF}	\mathcal{X}_B
Υ_{lu}	FLM	0.9488 (0.0034)	0.9491 (0.0034)	0.9484 (0.0032)
	FKNN	0.6044 (0.0274)	0.7550 (0.0165)	0.8805 (0.0078)
	FNN	0.9281 (0.0573)	0.9433 (0.0136)	0.9006 (0.0636)
Υ_{lb}	FLM	0.9486 (0.0031)	0.9491 (0.0035)	0.9492 (0.0034)
	FKNN	0.6046 (0.0203)	0.7556 (0.0134)	0.9258 (0.0052)
	FNN	0.8963 (0.0917)	0.9329 (0.0616)	0.9078 (0.0463)
Υ_{nl}	FLM	0.0111 (0.0113)	0.0108 (0.0116)	0.5820 (0.0531)
	FKNN	0.1108 (0.0437)	0.4303 (0.0330)	0.8828 (0.0093)
	FNN	0.5266 (0.0978)	0.8049 (0.0548)	0.8715 (0.0384)
Υ_d	FLM	0.6872 (0.0252)	0.6931 (0.0242)	0.6259 (0.0322)
	FKNN	0.4973 (0.0279)	0.6640 (0.0183)	0.8615 (0.0273)
	FNN	0.7136 (0.0841)	0.7197 (0.0705)	0.7506 (0.0477)

Table 4: Mean value (standard deviation) of $R^2(I)$ of FLM, FKNN and FNN for those scenarios with $m = 500$ and $\eta = 0.25$.

		\mathcal{X}_F	\mathcal{X}_{sF}	\mathcal{X}_B
Υ_{lu}	FLM	0.7432 (0.0180)	0.7476 (0.0134)	0.7435 (0.0151)
	FKNN	0.4581 (0.0221)	0.5741 (0.0195)	0.6728 (0.0191)
	FNN	0.7247 (0.0513)	0.7300 (0.0427)	0.7122 (0.0458)
Υ_{lb}	FLM	0.7415 (0.0185)	0.7442 (0.0172)	0.7430 (0.0157)
	FKNN	0.4613 (0.0252)	0.5719 (0.0225)	0.7164 (0.0168)
	FNN	0.6979 (0.0637)	0.7253 (0.0564)	0.7165 (0.0357)
Υ_{nl}	FLM	0.0102 (0.0106)	0.0107 (0.0114)	0.4560 (0.0457)
	FKNN	0.0641 (0.0463)	0.2988 (0.0350)	0.6799 (0.0176)
	FNN	0.3975 (0.0758)	0.6285 (0.0463)	0.6788 (0.0369)
Υ_d	FLM	0.5387 (0.0284)	0.5385 (0.0277)	0.4838 (0.0312)
	FKNN	0.3739 (0.0303)	0.5049 (0.0237)	0.6500 (0.0308)
	FNN	0.5400 (0.0697)	0.5731 (0.0503)	0.5929 (0.0391)

References

- Aumann, R. J. (1964). Markets with a continuum of traders. *Econometrica* 32(1/2), 39–50.
- Aumann, R. J. and L. S. Shapley (1974). *Values of Non-Atomic Games*. Princeton University Press.
- Barber, R. F. and E. J. Candès (2015). Controlling the false discovery rate via knockoffs. *The Annals of Statistics* 43(5), 2055 – 2085.
- Barber, R. F. and E. J. Candès (2019). A knockoff filter for high-dimensional selective inference. *The Annals of Statistics* 47(5), 2504 – 2537.
- Barredo Arrieta, A., N. Díaz-Rodríguez, J. Del Ser, A. Bennetot, S. Tabik, A. Barbado, S. Garcia, S. Gil-Lopez, D. Molina, R. Benjamins, R. Chatila, and F. Herrera (2020). Explainable artificial intelligence (xai): Concepts, taxonomies, opportunities and challenges toward responsible ai. *Information Fusion* 58, 82–115.
- Berrendero, J. R., A. Cuevas, and J. Torrecilla (2016). The mrmr variable selection method: a comparative study for functional data. *Journal of Statistical Computation and Simulation* 86(5), 891–907.
- Biecek, P. and T. Burzykowski (2021). *Explanatory model analysis: Explore, explain and examine predictive models*. Chapman and Hall/CRC.
- Boj, E., P. Delicado, and J. Fortiana (2010). Distance-based local linear

- regression for functional predictors. *Computational Statistics and Data Analysis* 54(2), 429–437.
- Borggaard, C. and H. H. Thodberg (1992, 3). Optimal minimal neural interpretation of spectra. *Analytical Chemistry* 64(5), 545–551.
- Breiman, L. (2001). Statistical modeling: The two cultures. *Statistical Science* 16, 199–231.
- Carrizosa, E., J. Ramírez-Ayerbe, and D. Romero Morales (2024, 12). A new model for counterfactual analysis for functional data. *Advances in Data Analysis and Classification* 18(4), 981–1000.
- Cohen, S., G. Dror, and E. Ruppin (2007, 7). Feature selection via coalitional game theory. *Neural Computation* 19(7), 1939–1961.
- Delicado, P. and D. Peña (2023). Understanding complex predictive models with ghost variables. *TEST* 32, 107–145.
- Ding, C. and H. Peng (2005, April). Minimum redundancy feature selection from microarray gene expression data. *Journal of Bioinformatics and Computational Biology* 03(02), 185–205.
- Feldman, B. E. (2005). Relative importance and value. *SSRN Electronic Journal*.
- Ferraty, F. and P. Vieu (2006). *Nonparametric Functional Data Analysis: Theory and Practice*. Springer Series in Statistics. Springer New York.
- Hall, P., H.-G. Müller, and J.-L. Wang (2006). Properties of principal component methods for functional and longitudinal data analysis. *The Annals of Statistics* 34(3), 1493 – 1517.
- Hall, P., D. S. Poskitt, and B. Presnell (2001). A functional data—analytic approach to signal discrimination. *Technometrics* 43(1), 1–9.
- Harris, C. R., K. J. Millman, S. J. van der Walt, R. Gommers, P. Virtanen, D. Cournapeau, E. Wieser, J. Taylor, S. Berg, N. J. Smith, R. Kern, M. Picus, S. Hoyer, M. H. van Kerkwijk, M. Brett, A. Haldane, J. F. del Río, M. Wiebe, P. Peterson, P. Gérard-Marchant, K. Sheppard, T. Reddy, W. Weckesser, H. Abbasi, C. Gohlke, and T. E. Oliphant (2020, 7). Array programming with NumPy. *Nature* 585(7825), 357–362.
- Hart, S. and A. Neyman (1988). Values of non-atomic vector measure games: Are they linear combinations of the measures? *Journal of Mathematical Economics* 17(1), 31–40.
- Heinrichs, F., M. Heim, and C. Weber (2023). Functional neural networks: shift invariant models for functional data with applications to eeg classification. In *Proceedings of the 40th International Conference on Machine Learning, ICML’23*. JMLR.org.

- Horváth, L. and P. Kokoszka (2012). *Inference for functional data with applications*. Springer.
- Kannai, Y. (1966). Values of games with a continuum of players. *Israel Journal of Mathematics* 4(1), 54–58.
- Kokoszka, P. and M. Reimherr (2017). *Introduction to Functional Data Analysis*. CRC Press.
- Lipovetsky, S. and M. Conklin (2001, 10). Analysis of regression in game theory approach. *Applied Stochastic Models in Business and Industry* 17(4), 319–330.
- Masís, S. (2021). *Interpretable Machine Learning with Python*. Packt Publishing Ltd.
- Masoumian Hosseini, M., S. T. Masoumian Hosseini, K. Qayumi, S. Hosseinzadeh, and S. S. Sajadi Tabar (2023, nov). Smartwatches in health-care medicine: assistance and monitoring; a scoping review. *BMC Med. Inform. Decis. Mak.* 23(1), 248.
- Molnar, C. (2022). *Interpretable Machine Learning* (2 ed.). <https://christophm.github.io/interpretable-ml-book/>.
- Neyman, A. (1994). Value of games with a continuum of players. In J. Mertens and S. Sorin (Eds.), *Game-Theoretic Methods in General Equilibrium Analysis*, NATO Science Series D:, Chapter VI, pp. 67–79. Springer Netherlands.
- Python Core Team (2019). *Python: A dynamic, open source programming language*. Python Software Foundation.
- Ramos-Carreño, C., J. L. Torrecilla, M. Carbajo Berrocal, P. Marcos Manchón, and A. Suárez (2024, 5). scikit-fda: A Python Package for Functional Data Analysis. *Journal of Statistical Software* 109(2), 1–37.
- Ramsay, J. and B. Silverman (2005). *Functional Data Analysis*. Springer Series in Statistics. Springer.
- Rao, A. R. and M. Reimherr (2023). Nonlinear functional modeling using neural networks. *Journal of Computational and Graphical Statistics* 32(4), 1248–1257.
- Shapley, L. S. (1953). A value for n-person games. In H. W. Kuhn and A. W. Tucker (Eds.), *Contributions to the Theory of Games II*, pp. 307–317. Princeton: Princeton University Press.
- Shapley, L. S. (1961). *Values of Games With Infinitely Many Players*. Santa Monica, CA: RAND Corporation.
- Székely, G. J., M. L. Rizzo, and N. K. Bakirov (2007). Measuring and testing dependence by correlation of distances. *The Annals of Statistics* 35(6), 2769 – 2794.

- Winter, E. (2002). The shapley value. In R. Aumann and S. Hart (Eds.), *Handbook of Game Theory with Economic Applications* (1 ed.), Volume 3, Chapter 53, pp. 2025–2054. Elsevier.
- Yao, J., J. Mueller, and J.-L. Wang (2021). Deep learning for functional data analysis with adaptive basis layers. In *International Conference on Machine Learning*, pp. 11898–11908. PMLR.